Electric field analysis and evaluation of a Cryogenic Bus bar for the IZEA Aircraft Power Distribution System

M. Tahir Khan Niazi[1,2*], Peter Cheetham[1,2]

[1] FAMU-FSU College of Engineering, Tallahassee, Fl 32310
[2] Center for Advanced Power Systems, Tallahassee, Fl 32310

[*]E-mail: mn19j@fsu.edu

Abstract. This paper presents the design and experimental evaluation of electrically insulating spacers for cryogenic busbars with anticipated voltage rating up to ± 3 kV DC. It is envisioned these busbars will be part of IZEA aircraft power distribution system. The design of the insulating spacer must account for physical, electrical, and thermal constraints. Three insulating spacer designs were developed where both poles of the busbar were installed within the same cryostat. The insulating spacer ensures sufficient standoff between each pole as well as the inner wall of the cryostat. Additionally, the insulating spacer has large openings to enable a cryogen to flow through the cryostat and to minimize pressure drop along the component. For each design a 3-D finite element model was developed to assess electric field enhancement around the insulating spacer and the results ranged from 0.6- 1.2 kV/mm when a notional 1 kV was applied. The electric field model showed feasibility of the design and room temperature partial discharge measurements were performed as experimental verification. Partial discharge values were recorded between 4 – 5.5 kV AC rms in 2.0 MPa helium gas at room temperature. The room temperature verifies the design and enable cryogenic measurements to be performed in the near future where higher partial discharge values are expected due to the increase dielectric strength of helium gas at cryogenic temperatures.

1. Introduction

The electrification of aviation represents one of the most significant technological paradigms in modern aerospace engineering, fundamentally reshaping how aircraft power systems are conceived and implemented [1]. This transformation is primarily motivated by environmental sustainability goals and the pressing need to achieve carbon neutrality in the aviation sector by 2050 [2]. Current projections indicate that the electric aircraft market will experience exponential growth, with estimates suggesting a market value exceeding $27.7 billion by 2030 [3].

Recent developments in electric propulsion have successfully validated the concept for smaller aircraft, with notable examples including the Pipistrel Alpha Electro trainer and Heart Aerospace's ES-30 regional aircraft [4,5]. However, the transition to larger commercial aircraft presents unprecedented engineering challenges, particularly in the realm of electrical power distribution where megawatt-level power handling capabilities are required [6,7]. These systems

must simultaneously achieve exceptional power density, maintain stringent weight limitations, and operate reliably under diverse environmental conditions.

Recognizing these challenges, the NASA University Leadership Initiative (ULI) " Integrated Zero Emission Aviation (IZEA)" focuses on developing high temperature superconducting (HTS)power distribution architectures capable of supporting 16 MW hybrid electric aircraft [8]. Initial trade-off studies within this program have identified various topologies utilizing HTS cables that achieve the target power density threshold of 25 kW/kg. These analyses have revealed that auxiliary components, particularly cryostats, terminations, and cryogenic transfer lines, constitute a significant portion of the overall system weight, potentially limiting the practical implementation of these technologies [9].

Recent research in this regard has explored the integration of HTS cables with cryogenic busbars as a means of achieving system-level optimization for aircraft power distribution[10]. This approach offers the potential to eliminate multiple HTS cable terminations, replacing 16 individual termination points with 4 consolidated cryogenic busbars in the IZEA light configuration. Such consolidation not only reduces system complexity but also provides opportunities for weight reduction and improved reliability.

Central to the successful implementation of cryogenic busbar systems is the design of insulating spacers that maintain proper conductor positioning while ensuring electrical isolation within the cryogenic environment. These components must satisfy multiple competing requirements: precise geometric positioning within confined spaces, electrical insulation under high voltage conditions, facilitation of cryogen circulation for thermal management, and minimization of electric field perturbations that could compromise system voltage ratings [11]. The interdependence of these requirements makes spacer design a critical aspect of overall system optimization.

This investigation presents a systematic approach to spacer design optimization for cryogenic busbar applications in electric aircraft. The methodology combines theoretical analysis based on COMSOL modelling and simulation of the spacer to predict electric field distributions and identify optimal geometric configurations. Experimental validation using representative material and operating conditions provides verification of analytical predictions and enables refinement of design parameters.

2. IZEA Aircraft's Power System

The IZEA aircraft employs a hybrid wing body (HWB) architecture designed to accommodate 112 passengers over an operational range of 2300 nautical miles. The IZEA light propulsion system features a distributed electric architecture incorporating 8 individual motor units, each delivering 2 MW of propulsive power. Power generation is achieved through a hybrid configuration combining two 8 MW HTS generators (providing 16 MW total capacity) with an auxiliary 2 MW fuel cell system, all interconnected via a DC distribution network linking the generation sources to the propulsive units. The power distribution of the IZEA light architecture enables the cryogenic busbar to be fed from either HTS generator while ensuring that each motor receives power from two different bus bars. This topology increases the redundancy and flexibility of the power system, critical for aviation safety requirements. The system architecture includes terminations at the interface between the generator rectifier and HTS cable, as well as between the HTS cable and cryogenic busbar. The main bus voltage of the DC distribution system is 800 V (± 400 V), which equates to the busbar having a maximum operating current of up to 5 kA during take-off conditions. During cruise operation, which constitutes the majority of flight time, the

busbar is expected to operate at approximately 2.5 kA. For the IZEA light configuration, there are 16 termination points with 1 MW rating, approximately 0.5-1 m apart from one another.

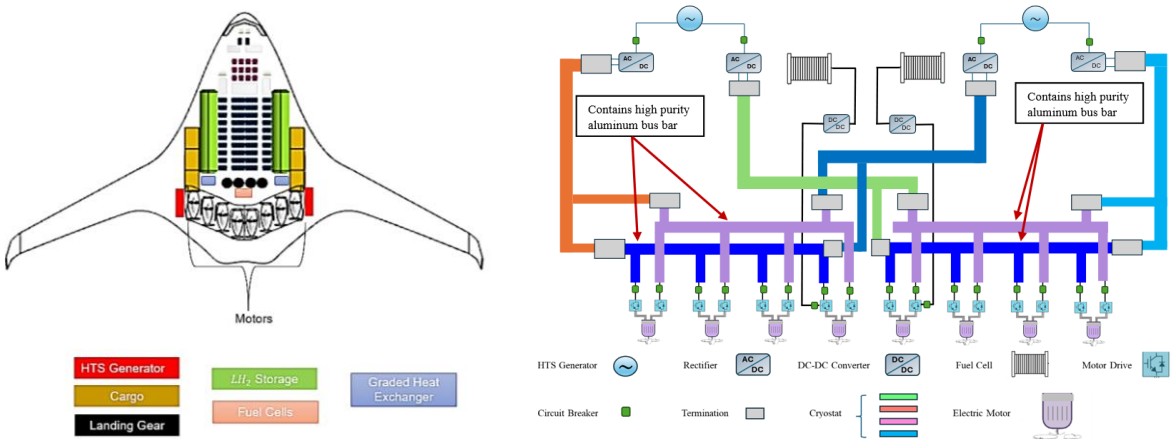

(a) (b)

Figure 1. IZEA aircraft (a) IZEA layout, (b) IZEA power system

3. Cryogenic Bus Bar

When developing a notional busbar design it was seen advantageous to determine a material which could support current densities within the range of 2.5-5 A/mm^2 and identify quick electrical connectors which can support these current levels at cryogenic temperatures. These design assumptions enable a cryostat size to be selected as part of the initial conceptual design. From review of commercial cryostats, the R300 from Technifab [12] was identified as a potential option. This cryostat has an inner diameter of 85.6 mm and would support two busbars with dimensions of 1.75 in x 1 inch (44 mm x 25 mm) equating to a cross-sectional area of ~1100 mm^2. Based on fitting two poles within one cryostat the standoff between each pole as well as the cryostat to ranges between 4-8 mm. This clearance should be sufficient to achieve the intended operating conditions of ± 400 V and enable voltage up to ± 3 kV [13,14].

The main bus is connected to feeder buses which supply power to the 1 MW load and the feeder bus has dimensions of 1.57 inch x 0.375 inch (40 mm x 9.5 mm) equating to a cross sectional area of ~380 mm^2. Additional details on how the connection between the main bus and feeder bus are made using multilam connectors is provided in [10]. The smaller dimensions of the feeder bus allow for larger standoff distances between each pole as well as the cryostat to be achieved compared to the main bus. This highlights that the electrical standoff achieved by the

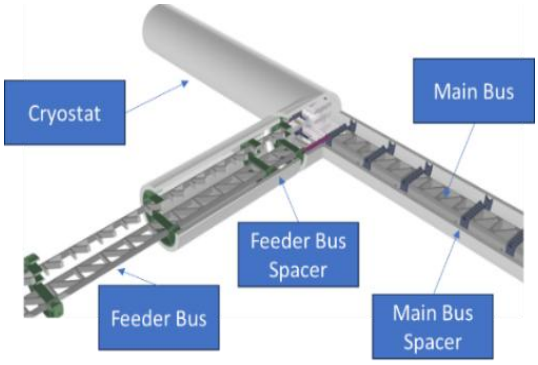

Figure 2. Complete bus bar assembly

main bus spacer represents the location of highest electric field stress within the busbar design. As such the design and verification of the electrical insulating spacer for the main bus was seen as an important milestone to determine the feasibility of the cryogenic busbar.

3.1 Fundamental Spacer Design Considerations

The design of insulating spacers for cryogenic busbars presents unique challenges that differ significantly from conventional room-temperature applications. The spacer must fulfill multiple critical functions while operating in the cryogenic environment which includes maintaining the conductor position within the cryostat to enable connection to the feeder bus, providing electrical isolation between the conductor and grounded cryostat wall, and enabling cryogen circulation for thermal management. The spacer design should minimize electric field enhancement that could lead to dielectric breakdown occurring.

The operating temperature and pressure of the helium gas will influence the electrical performance of the busbar. The operating temperature of the helium gas will influence the electrical resistance of the busbar which in turn will dictate the heat load being produced. The density of the helium gas will influence the achievable mass flow rate of the helium gas as part of the closed loop thermal circulation system. The dielectric strength of the helium gas is also a function of density and at cryogenic temperatures dielectric strengths between 4-8 kV/mm can be anticipated [13]. For cryogenic application operating pressure up to 2 MPa are common, and it is the maximum allowable working pressure of the R300 cryostat which is the basis of design of the cryogenic busbar. The operating temperature of the cryogenic busbar is expected to be between 70-120 K based on the system level optimization of the IZEA power distribution system [9,10]. The cryogenic busbar couples between the HTS cable (50-70 K) and the motor drives (110-130 K). For different power system configuration lower operating temperatures of the cryogenic busbar will be possible to reduce the electrical resistance of the busbar and enabling higher operating currents.

The spacing between individual spacers along the busbar length represents a critical design parameter that must balance mechanical support requirements with weight optimization. Based on the physical dimensions and structural loading conditions, spacers are positioned at intervals determined by the maximum allowable conductor deflection under electromagnetic and thermal stresses. For the proposed busbar configuration with termination points spaced 0.5-1 m apart, intermediate spacers may be required at similar intervals to prevent excessive conductor movement and maintain concentricity within the cryostat. Based on the dimensions of the IZEA light aircraft each busbar is expected to have an overall length between 4-5 m. Additional spacers may be required near the connection point between the main bus and feeder bus to assist in alignment as shown in Figure 2.

The selection of appropriate materials for cryogenic busbar spacers requires consideration of multiple properties that interact in complex ways. The relative permittivity and electrical conductivity of the spacer material will influence the electric field around the spacer. DC electric fields are a function of relative permittivity and electrical conductivity when a device is first energized and influence the time required for a steady state DC electric field to be established. A steady state DC electric field is a function of the electric conductivity. The electric field profiles under a transient DC electric field and a steady state DC electric field can have different electric field magnitudes and locations of highest electric field enhancement. To accurately model the DC electric field requires the electrical conductivity of the spacer material to be measured at cryogenic temperature as the electrical conductivity of a material can change by an order of

magnitude between room and cryogenic temperatures [15]. Accurate materials properties in turn lead to accurate electric field simulations being developed.

The geometric constraints imposed by the 85.6 mm cryostat inner diameter necessitate spacer designs that maximize available flow area for cryogen circulation while providing adequate mechanical support and electrical insulation. The feeder bus interfaces, which must accommodate quick electrical connections for the 16 termination points, further constrain the spacer geometry and require integration of low-resistance electrical couplings compatible with cryogenic operation. These design constraints collectively define the operational envelope within which spacer optimization must be achieved.

3.2 Electric Field Distribution and Enhancement

The presence of insulating spacers within the cryogenic busbar system inevitably creates electric field triple points which occur at the interface between the busbar, spacer, and cryogen. The triple points can lead to localized electric field enhancement that may limit the voltage rating of the entire system and increase the probability of partial discharges at these locations. The magnitude of this enhancement depends on several factors: the geometry of the spacer, the mismatch in the electrical properties between the spacer material and cryogen, and the specific location and design of any openings required for cryogen circulation.

Building upon the understanding of electric field enhancements in cryogenic busbar systems, three distinct spacer design configurations were developed for comprehensive evaluation. Figure 3 illustrates the geometric variations under consideration: (a) a dual-pole design with rectangular openings for cryogen flow (spacer A), (b) a similar dual-pole configuration with modified opening geometry (spacer B), and (c) a circular design featuring distributed perforation patterns around the circumference (spacer C). Each design represents a different approach to balancing the competing requirements of mechanical support, electrical insulation, and thermal management within the constrained geometry of the cryogenic busbar system. The thermal concerns will be explored in greater detail in future publications.

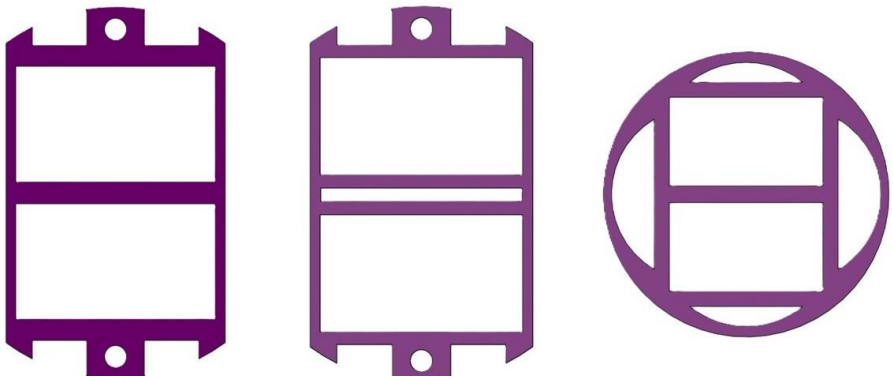

(a) Spacer A (b) Spacer B (c) Spacer C

Figure 3. Spacer designs

Figure 4a demonstrates the integration of a spacer design within the complete busbar assembly, along with the cross-sectional view (Figure 4b).

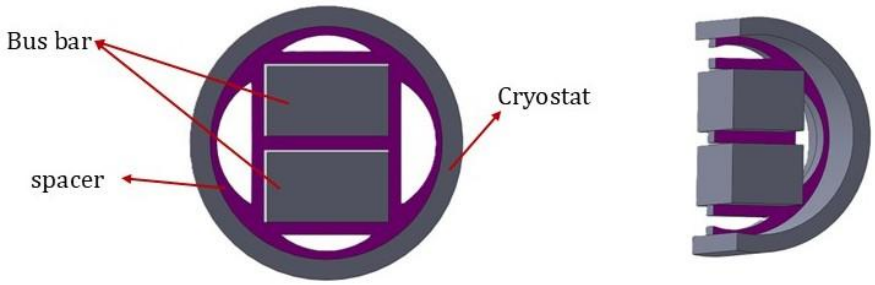

(a) (b)

Figure 4. Spacer along with bus bar assembly, (b) section view

Electric field analysis was conducted using COMSOL Multiphysics to quantify the electrostatic performance of each spacer configuration under representative operating conditions. The electric field analysis focused on ac electric fields which represent the electric field gradient observed when the busbar is first energized. For performing the electric field simulation, G-10Cr with relative permittivity (ε_r) 4 was chosen as it has good material compatibility with cryogenic temperatures. The simulation domain encompassed the complete coaxial geometry, including the bus bar conductors, insulating spacer, cryogen-filled regions (gaseous helium), and grounded cryostat wall. The top busbar was assigned a voltage of 1 kV, the bottom busbar was assigned a voltage of -1 kV and the cryostat was set to ground voltage. The remaining volume within the cryostat which was not occupied by the busbars or the spacer was given ε_r value of 1 to represent helium gas. Figure 5 presents the electric field distribution results for the three spacer configurations.

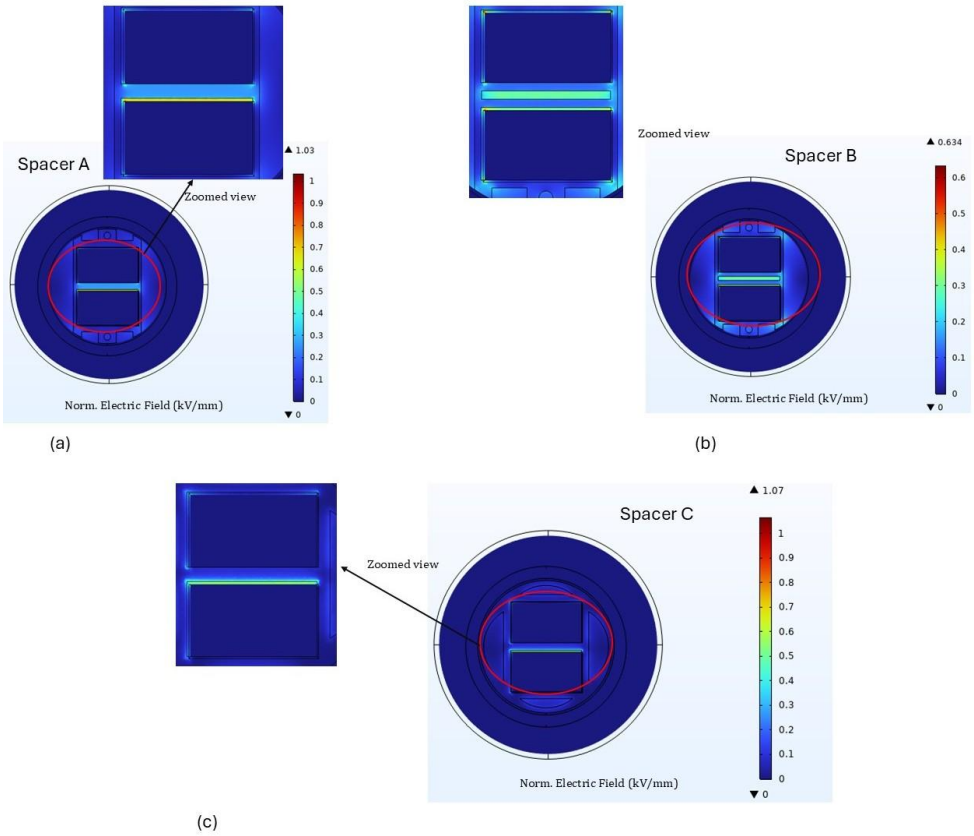

Figure 5. Electric stress (kV/mm) analysis of spacer design

Figure 5 shows that the electric field gradient ranges from 0.6 – 1.07 kV/mm. The region of highest electric field stress occurs between the top and bottom electrode. The electric field enhancement is caused due to the opening of the spacer being slightly larger than the busbar dimension to allow it to be installed. This small gap is filled with helium gas and due to the mismatch in permittivity between the G-10Cr and helium gas electric field enhancement occurs within this region. The electric field results show similar field profiles between Spacer A and Spacer C and based on these results the DC models for Spacer C were developed.

The DC transient models utilized the same geometry as shown above. The DC models had ± 1 kV applied to the busbars and had the cryostat set to ground potential. The transient model used the same permittivity values as the AC model and used electrical conductivity values for the helium gas and G-10Cr at 77K which have previously been reported in [16]. The DC transient electric field model was simulated for a 5-hour time period which reflects the maximum flight duration of the IZEA light aircraft. The results of the DC transient for every 5 minutes of the 5-hour flight is shown in Figure 6.

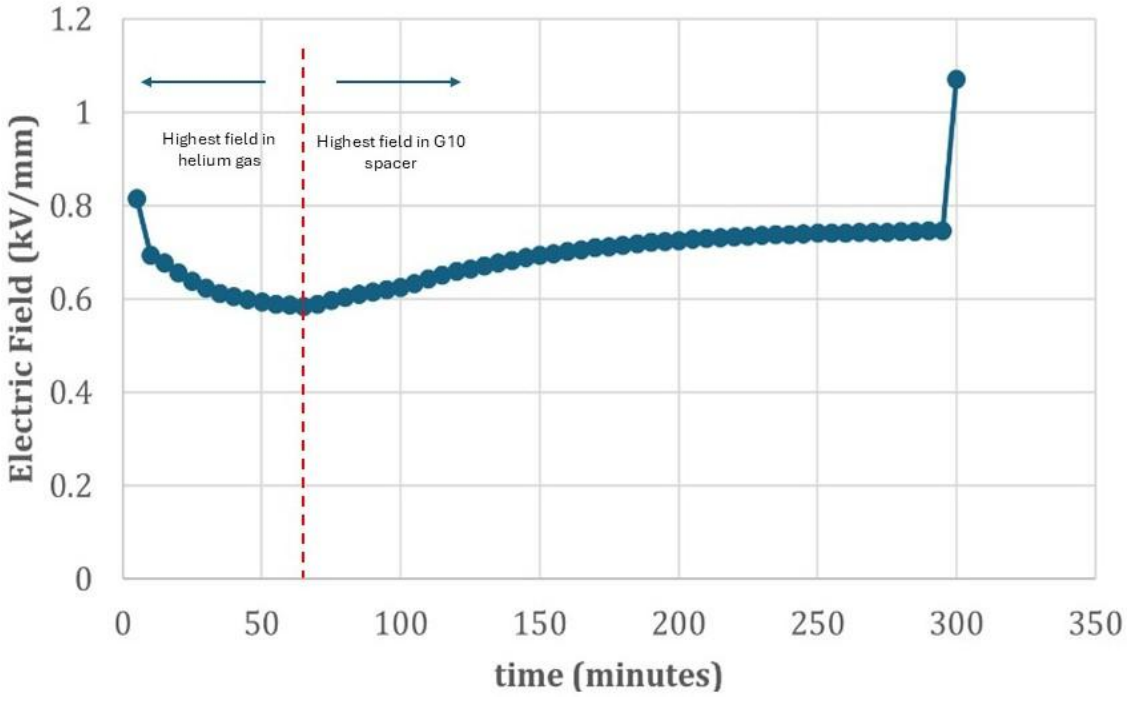

Figure 6. DC Electric field variation with time over a period of 5 hour for spacer c

Figure 6 shows that the highest electric field within the setup occurs within the helium gas for the first 60 minutes after the busbar is energized. After 60 minutes the maximum electric field occurs within the G10 spacer. Based on the conductivity values, a steady state DC electric field is not expected to be established until 14 hours. The peak in electric field at 300 minutes is based on the voltage supply being turned off within the model and represents the start of the de-polarization stage of the DC electric field.

4. Experimental Setup

In order to verify the electric field simulation results, an experimental setup was employed to investigate partial discharge behavior of the insulating spacers based on the geometrical

constraints of the cryogenic busbar. For the experimental setup two spacers were fabricated using the design shown for Spacer C. Two aluminum bus bar conductors with cross section of 1.75 in x 1 inch and length of 14.5 inches were installed within the spacers (Figure 7a) and then installed within a stainless-steel tube with an inner diameter of 85 mm and length of 12 inches (Figure 7b). The completed assembly was placed within a ConFlat hardware by joining two 8-inch ConFlat (CF) Tee pressure vessels to establish the full test enclosure. 30 kV rated high voltage bushing were connected on each end of the pressure vessel with one bushing connected to each aluminum bubsar. Both the stainless-steel enclosure and pressure vessel were connected to ground. Additional gas hardware was added to the experiment setup to enable pumping, purging and filling cycles to be completed on the experimental setup. These steps have been previously outlined in [17]. From completing these steps, the experimental setup established a high purity helium gas environment at 2.0 MPa at room temperature.

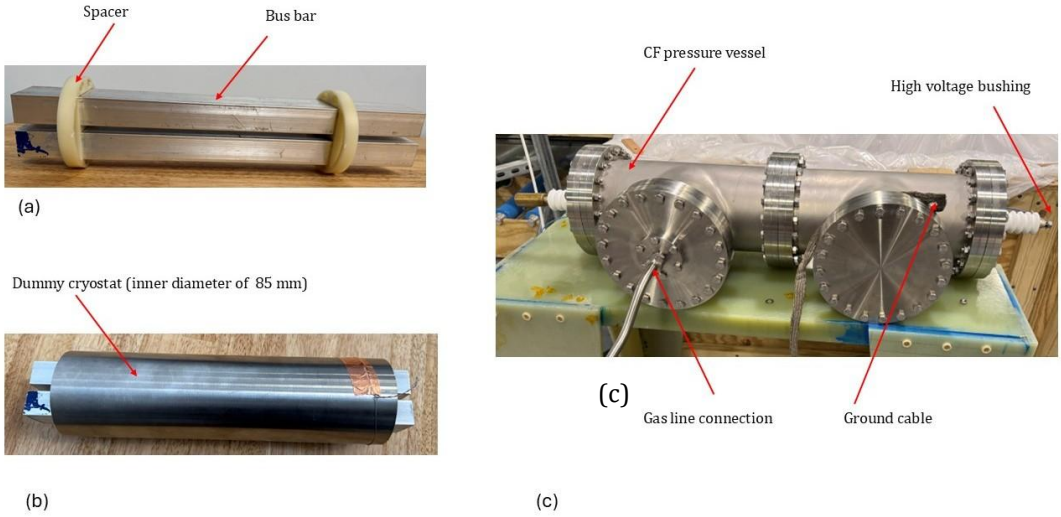

Figure 7. Experimental setup for partial discharge measurement setup

5. Partial Discharge (PD) Measurement

Partial discharge measurements were conducted within the Faraday Cage at the Center for Advanced Power Systems (CAPS) which has a background noise floor of 0.5 pC. The experimental setup was connected to a 100 kV, 5 kVA, ac transformer test circuit which also included a partial discharge coupling capacitor. The high voltage circuit allowed for one of the high voltage bushings/busbar poles to be energized while the other high voltage bushing/busbar pole is connected to ground potential. Once partial discharge measurements were completed on one configuration the experimental connections were swapped. For all configuration the stainless-steel tubing/CF hardware was at ground potential.

Partial discharges were recorded using an Omicron MPD 800 and before the experiments were conducted the experimental setup was calibrated to 20 pC utilizing a MPD 542 calibration unit. When performing the partial discharge measurement, the voltage applied to the experimental setup was increased in increments of 300 V. At each voltage step the partial discharge activity was observed and when partial discharge activity continuously exceeded 10 pC, the partial discharge inception voltage (PDIV) was recorded. Once at PDIV the experimental setup was held for at this voltage level for one minute to record the phase resolved partial discharge (PRPD) pattern. The PRPD pattern gives insight on the type of partial discharge occurring within the system. Once the PRPD pattern was recorded the voltage was reduced in steps of 300 V until

the partial discharge activity ceased which is referred to as the partial discharge extinction voltage (PDEV). A summary of the PDIV and PDEV of the experimental setup in helium gas at 2.0 MPa at room temperature is shown below in Table 1.

Table 1 shows a ~25 % reduction in partial discharge inception voltage when the bottom busbar is connected to the HV power supply compared to when the top busbar is connected to the HV power supply. This is the expected result as for this configuration the electric field enhancement within the helium gas which fills the gap between the busbar and spacer will be higher. Overall, the results show the feasibility of this cryogenic busbar to be rated for ±400 V.

Table 1. PDIV and PDEV values for chosen spacer

Experimental Configuration		**Test**	**PDIV (kV ac rms)**	**PDEV (kV ac rms)**
Top Busbar Pole	Bottom Busbar pole			
HV	Ground	Run 1	5.5	4.13
		Run 2	5.3	4.12
Ground	HV	Run 1	4.2	3.07
		Run 2	3.96	3.3

6. Discussion

Future work to be completed on this experimental setup is to repeat this measurement in helium gas at 77 K and pressures ranging from 0.5-2.0 MPa. It is expected that the PDIV values recorded at 0.5 MPa and 77 K will be similar in magnitude to the values obtained at 2.0 MPa and room temperature as the density of helium gas at these two conditions are equivalent to one another. As the pressure is increased at 77 K, higher PDIV values are expected due to the higher density of the helium gas.

We also plan to complete the measurement under DC voltage for both room and cryogenic temperatures. This will enable a greater understanding of the electric field profile of the busbar under relevant operating conditions of the IZEA aircraft to be studied.

7. Conclusion

This study evaluated spacer designs for cryogenic busbars in electric aircraft applications through combined simulation and experimental approaches. COMSOL analysis demonstrated the difference in electric field profile under ac and transient dc conditions of the cryogenic busbar.

Experimental partial discharge testing using individual pole energization revealed PDIV values of 5.3-5.5 kV for the top busbar pole and 3.96-4.2 kV for the bottom pole at room temperature in gaseous helium. Both configurations significantly exceed the proposed 800 V operating voltage, providing substantial safety margins. The performance variation between pole positions emphasizes the importance of comprehensive interface testing within the busbar assembly.

Further measurements are to be conducted at cryogenic conditions, at 77 K, using a DC power supply for the complete characterization of the spacers.

Acknowledgments
This research was funded by the NASA University Leadership Initiative (ULI) #80NSSC22M0068.

References

[1] Benzaquen J, He J and Mirafzal B 2021 Toward more electric powertrains in aircraft: Technical challenges and advancements *CES Trans. Electr. Mach. Syst.* **5** 177–93

[2] Jensen L L, Bonnefoy P A, Hileman J I and Fitzgerald J T 2023 The carbon dioxide challenge facing U.S. aviation and paths to achieve net zero emissions by 2050 *Prog. Aerosp. Sci.* **141** 100921

[3] Anon Electric Aircraft Market to Reach $27.7-Billion by 2030 | Aero-News Network

[4] Anon 2015 Pipistrel Alpha Electro: The trainer of the future?

[5] Anon Heart Aerospace Unveils First Full-Scale Demonstrator for 30-seat Hybrid-Electric Airplane | Heart Aerospace

[6] Cano T C, Castro I, Rodríguez A, Lamar D G, Khalil Y F, Albiol-Tendillo L and Kshirsagar P 2021 Future of Electrical Aircraft Energy Power Systems: An Architecture Review *IEEE Trans. Transp. Electrification* **7** 1915–29

[7] Anon Next Generation More-Electric Aircraft: A Potential Application for HTS Superconductors | IEEE Journals & Magazine | IEEE Xplore

[8] Wellock B 2022 NASA selects FAMU-FSU College of Engineering to help develop sustainable aviation system *Fla. State Univ. News*

[9] Niazi M T M K and Cheetham P 2024 Evaluation of Power Distribution Architectures for the IZEA Fleet *AIAA AVIATION FORUM AND ASCEND 2024* AIAA Aviation Forum and ASCEND co-located Conference Proceedings (American Institute of Aeronautics and Astronautics)

[10] Niazi M T K, Kim C H and Cheetham P 2025 Cryogenic Bus Bar Design for IZEA Aircraft Power Distribution System *2025 IEEE/AIAA Transportation Electrification Conference and Electric Aircraft Technologies Symposium (ITEC+EATS)* 2025 IEEE/AIAA Transportation Electrification Conference and Electric Aircraft Technologies Symposium (ITEC+EATS) pp 1–6

[11] Anon Electric field analysis of insulating spacers for a superconducting gas-insulated transmission line | IEEE Conference Publication | IEEE Xplore

[12] Anon Techniguard R-Series *Tech. Prod. Inc*

[13] Cheetham P, Kim W, Kim C H, Graber L, Rodrigo H and Pamidi S 2016 Enhancement of dielectric strength of cryogenic gaseous helium by addition of small mol% hydrogen *IEEE Trans. Appl. Supercond.* **27** 1–5

[14] Cheetham P, Viquez J, Graber L, Kim C H, Rodrigo H and Pamidi S 2017 Novel Design Concept and Demonstration of a Superconducting Gas-Insulated Transmission Line *IEEE Trans. Appl. Supercond.* **27** 1–5

[15] Das A K, Guvvala N, Cheetham P and Pamidi S 2025 Measurement and Modelling of Time Domain Dielectric Response of Insulating Materials at Cryogenic Temperature *IEEE Trans. Dielectr. Electr. Insul.* 1–1

[16] Kasen M B, MacDonald G R, Beekman D H and Schramm R E 1980 Mechanical, Electrical, and Thermal Characterization of G-10Cr and G-11Cr Glass-Cloth/Epoxy Laminates Between Room Temperature and 4 K *Advances in Cryogenic Engineering Materials: Volume 26* ed A F Clark and R P Reed (Boston, MA: Springer US) pp 235–44

[17] Mensah P, Martin S, Guvvala N, Cheetham P and Pamidi S V 2025 Electric Field Analysis and Partial Discharge Measurements-Aided Design of Electrical Insulation Systems for HTS Cables for Electric Transportation *IEEE Trans. Appl. Supercond.* **35** 1–5